BJRS

BRAZILIAN JOURNAL
OF
RADIATION SCIENCES
08-03 (2020) 01-16

SBPR
Sociedade Brasileira de Proteção Radiológica

Evaluation of PETG as a material for immobilization device used in radiation therapy for head and neck

Birnfeld[a] H., Touguinha[b] G.C., Santos[c] R.R., Alva-Sánchez[d] M.S., Millão[e] L.

[a]*Master Programme in Health Education, Federal University of Health Sciences of Porto Alegre, CEP 90050-170, Porto Alegre, Rio Grande do Sul, Brazil*

[b]*Bachelor's degree programme in Medical Physics, Federal University of Health Sciences of Porto Alegre, CEP 90050-170, Porto Alegre, Rio Grande do Sul, Brazil*

[c]*Radiotherapy Department, Irmandade da Santa Casa da Misericórdia of Porto Alegre, CEP 90035-072, Porto Alegre, Rio Grande do Sul, Brazil*

[d]*Exact and SocialApplied Sciences Department, Federal University of Health Sciences of Porto Alegre, CEP 90050-170, Porto Alegre, Rio Grande do Sul, Brazil*

[e]*Nursing Department, Federal University of Health Sciences of Porto Alegre, CEP 90050-170, Porto Alegre, Rio Grande do Sul, Brazil*

heitor.birnfeld@gmail.com

ABSTRACT

In planning the radiotherapy treatment of head and neck cancer, the oncologist can indicate the use of an intraoral prosthesis to facilitate the radiation therapy planning and reduce the toxicity of the treatment. These devices are commonly fabricated with dental acrylic resin, the polymethylmethacrylate (PMMA), yet there are reports about manufacture in thermoplastic materials. The polyethylene terephthalate glycol (PETG) is a compound used for the fabrication of dental appliances, which could be used at intraoral prosthesis manufacture. The main objective of the present work was to evaluate the potential use of PETG at intraoral prosthesis for radiotherapy of head and neck cancer. Materials and methods: Circular forms of PMMA and PETG of thicknesses of 1, 2 and 3 mm were used with the dimensions of a head phantom, which allowed the insertion of a radiochromic film. The irradiations

ISSN: 2319-0612
Accepted: 2020-08-19

occurred at a linear accelerator with photons of 6 MeV energy. Results: The percentage depth dose differences of the materials PMMA and PETG were of 3%, 8% and 4%, respectively for the thicknesses of 1, 2 and 3 mm, around the position of the circular forms. Conclusion: Based on the results obtained, it can be inferred that PETG is suitable for manufacturing the intraoral prosthesis for radiotherapy treatment, replacing existing materials.

***Keywords*: Immobilizers, radiotherapy, PETG.**

1. INTRODUCTION

Head and neck cancer have a multimodal treatment, being surgery followed by radiotherapy the most common one amongst all therapeutic modalities [1]. As primary therapy, radiotherapy could be used in the first stages of the disease (T1 and T2 injury) with excellent local control and survival rate (85% to 90%) [2]. However, this treatment technique has some level of toxicity, what may affect basic functions such as chewing, swallowing, breathing, phonation and the senses (taste, smell, vision, and hearing). It also can alter one's physiognomy either transiently or permanently [3-5]. The most common oral adverse effects in patients submitted to radiotherapy are xerostomy, mucositis, dysgeusia, hypogeusia, opportunistic infections, trismus, radiation caries, dysphagia, and osteoradionecrosis [6,7].

For oral cavity, paranasal sinuses and pharynx cancer, the radiation oncologist may request the dental surgeon the production of intraoral prosthesis in order to facilitate the radiation therapy planning and may diminish treatment toxicity [3,4,8]. Immobilizers have the function of improving positional reproducibility and preventing patient movement during the application of radiotherapy [9], as in Figure 1.

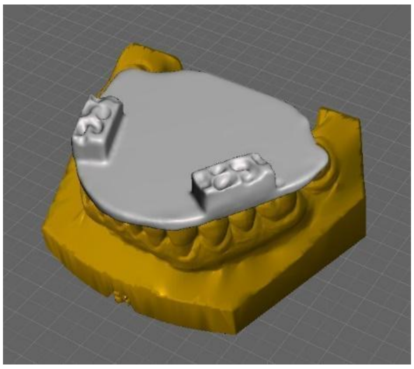

Figure 1: *Intraoral prosthesis for radiotherapy in 3d design in grey.*

According to Kaanders [10], intraoral prosthesis for radiotherapy can be categorized in two types: protective or positioning. Protective devices reduce the dose of radiation on healthy tissues, incorporating blocking materials in its structure. On the other hand, positioning devices can rearrange the tissues into a radiation field or move healthy tissues away, decreasing the volume of the radiation dose.

Most of intraoral prosthesis for radiotherapy are made of polymethylmethacrylate (PMMA), an acrylic resin used for laboratory techniques for dental prosthesis, presenting an atomic number close to that of the water, with excellent structural resistance [11-15]. Some authors have already described the use of thermoplastics to produce such devices, as ethylene vinyl acetate [16,17], polyester [18] and polyethylene terephthalate (PET) [19,20].

The PETG is a thermoplastic commonly used in odontology in the technique of vacuum thermoforming for the production of protective devices [21,22] and orthodontic devices [23,24], being biocompatible, resistant, easy to finish, low cost and with a simpler technique application when compared to PMMA. Despite clinical reports of the use of PET as intraoral radiotherapy positioners, no study was found regarding the use of PETG through a dosimetry evaluation.

A way of evaluating the usage behaviour of PETG in radiotherapy treatments is through an analysis of the percentage depth dose variations by using dosimeters with high spatial resolution, as radiochromic films.

A radiochromic film is a dosimeter that fits the method used in this experimental study once it has characteristics such as insensitivity to light, non-dependence on energy, high spatial resolution, amongst other characteristics [25,26]. When exposed to ionizing radiation, the structure of its sensitive crystalline material will modify in the form of polymerization of the monomers elements present in the film, resulting in alteration of the material's rate of visible light transmission. Such colour modification may be related to the exposed radiation dose [27-29].

The objective of the study is to verify the dosimetry behaviour of PETG, aiming its usage as a material for intraoral prosthesis in radiotherapy using radiochromic films.

2. MATERIALS AND METHODS

This experimental study occurred in the radiotherapy service of an oncology reference school-hospital in Porto Alegre, Rio Grande do Sul - Brazil.

For the study, two sets of circular disc plates containing three different thicknesses – 1, 2 and 3 mm – were used. One set of plates was manufactured using PETG (crystal plate – Bioart, Brazil) and the other set was manufactured using PMMA (self-curing jet – Clássico, Brazil), both obtained by using the following laboratory technique: the manufacture of PMMA plates was realized by duplicating PETG plates with 130 mm of diameter and thicknesses of 1, 2 and 3 mm – two plates of each – using the technique of inclusion in plaster.

Such technique was executed using type III plaster (Herodent – Coltene, Brazil). The PETG plates with thicknesses of 1, 2 and 3 mm were placed over a plain surface inside three 200 mm tubes of polyvinyl chloride (PVC) cut at the height of 6 cm. The plaster was poured over the three plates at the height of 2 cm. Finishing the total plaster setting (3 hours), the opposite part of the plate was turned up and isolated with solid Vaseline; the other portion of plaster was then poured at the height of 2 cm. After completing the plaster setting, the PETG plates were removed, a plaster mould being obtained as a result. That plaster mould, then, was isolated (Cel-Lac – SSWhite, Brazil) and the acrylic resin (PMMA) was elaborated following the manufacturer's guidance, being rested on the mould, pressed and put under the pressure of 20 psi using a polymerizing pot (Essence Dental – VH, Brazil). After 20 minutes, the resulting acrylic plate was removed from the plaster and sanded with 150, 200 and 400 grit finishing sandpaper, having its thickness confirmed by an analogue calliper (Vonder, Brazil). Thus, three plates corresponding to the PETG plates were obtained. The study was structured according to the following steps. The table 1 shows the physics properties from the materials studies and, also, soft tissue and water.

Table I: Table physics properties of PMMA and PETG [30-34].

	PETG[1]	PMMA	SOFT TISSUE	WATER

Density (g/cm^3)	1.27	1.19	1.04	1.00
Atomic effective number	6.62*	6,47	7.64	7.42

* The atomic effective number was calculated by the authors following the formulation proposed by Singh, V. P. et al [33].

[1] ttps://www.medicalexpo.com/pt/prod/bio-art-equipamentos-odontologicos/product-71548-866461.html

2.1. Experimental irradiation

The reference percentage depth dose in water was assessed using clinical dosimetry reference conditions obtained from the commissioning process applied to a Varian Unique Linear Accelerator present in the hospital, as in Figure 2. The reference conditions are photons beams of 6MV, 10x10 cm² field and distance of 100 cm from the source and the surface, irradiating a 30x30x30 cm³ water phantom. Since the commissioning, a periodic institutional quality assurance program ensures the dosimetry qualities of the equipment.

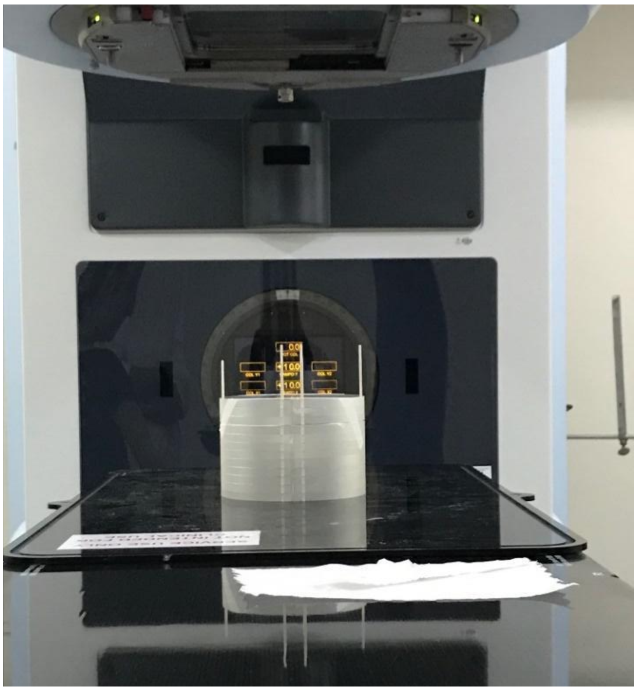

Figure 2: *Prepared phantom over the Varian Unique linear accelerator table.*

The PMMA head-simulating object – 21 cm high and 17 cm wide – has 1 cm high cuts divided in half, which facilitates the insertion parallel to the central axis of beam of the radiochromic film.

The PMMA and PETG plates were placed between the cuts of the simulator object 3 cm depth. For each irradiation, a type of immobilizer plate material was used, being the thickness of each one evaluated individually.

GafChromic® EBT 2 radiochromic films with 10x5 cm approximately were positioned in the central region of the irradiation field along the propagation of the irradiation beam. Figure 3 shows the setup of the irradiation with the film positioned parallelly along the beam axis.

The setup showed in Figure 2, contenting the film, was irradiated in same irradiation conditions as the reference percentage depth dose in water used in this work.

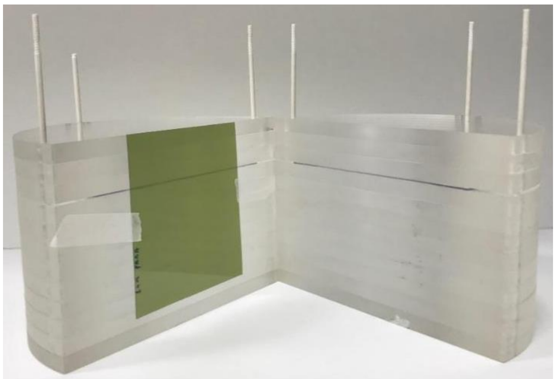

Figure 3: *Position of the radiochromic film in the head-simulating object.*

After the experimental irradiation, radiochromic films were digitized – within 24 hours after irradiation – in a personal use HP Photosmart D110 printer, following Marini's recommendations [35].

2.2. Data analysis process

The processing of the film's sign strength was realized using a software from Phyton platform – with a spatial resolution of 0.05 cm – that created curves from which profiles of percentage depth dose (PDD) were generated in the central axis of the radiation beam. To achieve such result only in the central axis, the mean of its 7 central columns was calculated to decrease errors.

Aside from determining dose profiles in the central axis, films sign strength data was used to calculate the percentage of relative dose, as in equation (1).

$$\%D = \frac{D}{D_{max}} 100\% \tag{1}$$

In which *PDD* is the percentage depth dose relative to the ratio between dose *D* in certain depth and dose D_{max} – dose maximum value.

For the central column, standard deviation calculations were made using a function from Phyton software – std – and of associated uncertainty at each point from the uncertainty propagation equation, as in equation (2).

$$\sigma_f = \sqrt{\left(\frac{\partial f}{\partial x}\right)^2 \sigma_x^2 + \left(\frac{\partial f}{\partial y}\right)^2 \sigma_y^2} \tag{2}$$

Considering f as a function that depends on variables x and y; $\frac{\partial f}{\partial x}$ and $\frac{\partial f}{\partial y}$ as partial derivatives from function f in relation to each one of its variables; and σ_f, σ_x and σ_y as the uncertainties of each variable.

The function used in the uncertainty propagation calculation was the percentage dose, as in equation (1).

This way, a variation of equation (1) was made and applied in the uncertainty propagation equation – equation (2). Lastly, σ_f represents the uncertainty of each point of the matrix.

With a code done for each radiochromic film, Microsoft® Office Excel was used to plot comparative charts. Those charts contain percentage depth dose information of plates with the same thickness of PMMA and PETG, so it becomes possible to evaluate all information and determine if there is any difference between materials. Yet, charts contain the parameter information, whose material is water.

3. RESULTS AND DISCUSSION

As a result for each of the 6 codes of each plate, a chart for 1, 2 and 3 mm thick plates was created – see Figure 4 for the chart corresponding to plates of 1 mm thick, Figure 5 for plates of 2 mm thick, and Figure 6 for plates of 3 mm thick.

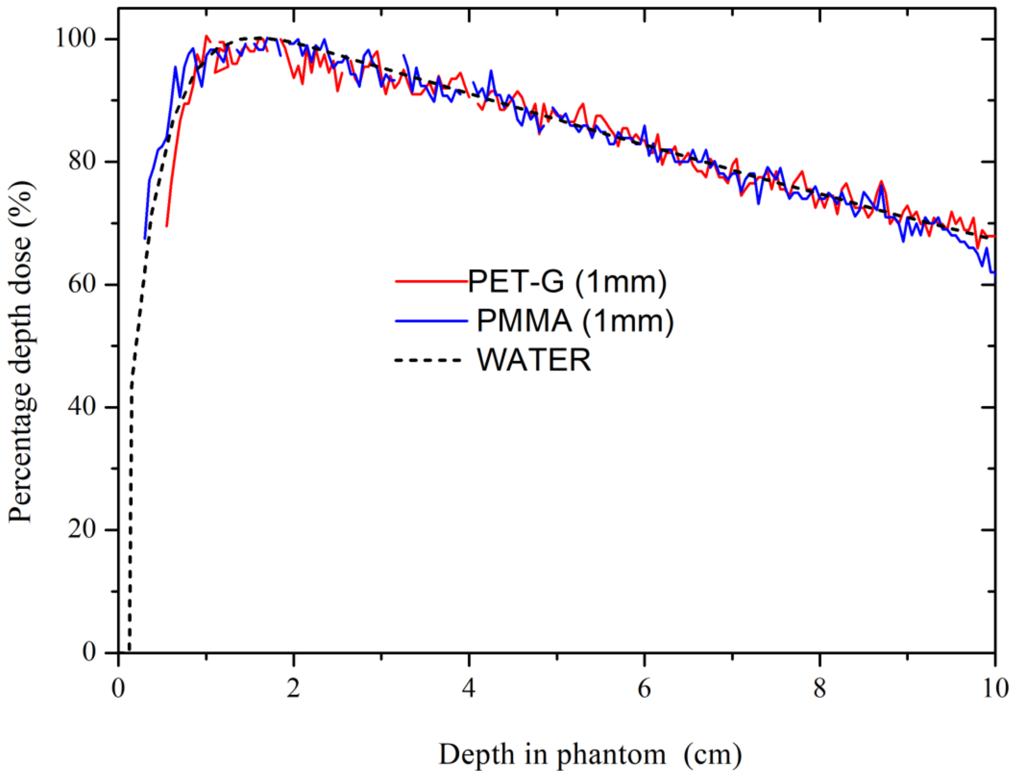

Figure 4: *Comparative chart for 1 mm thick PMMA and PETG plates.*

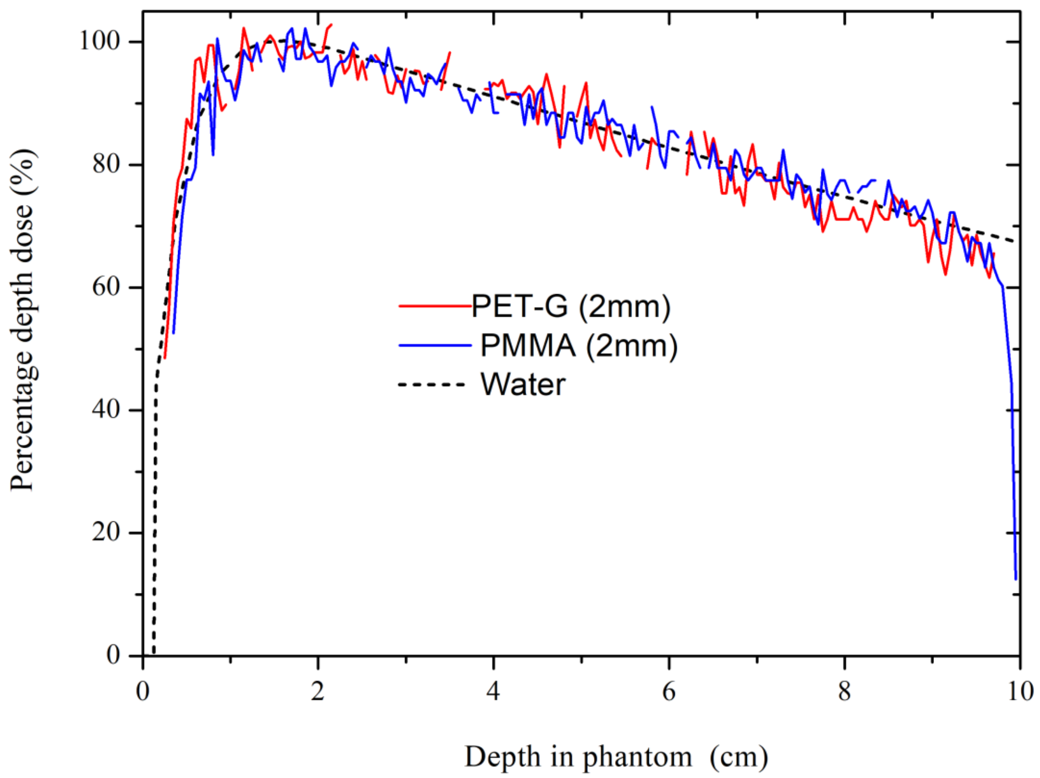

Figure 5: *Comparative chart for 2 mm thick PMMA and PETG plates.*

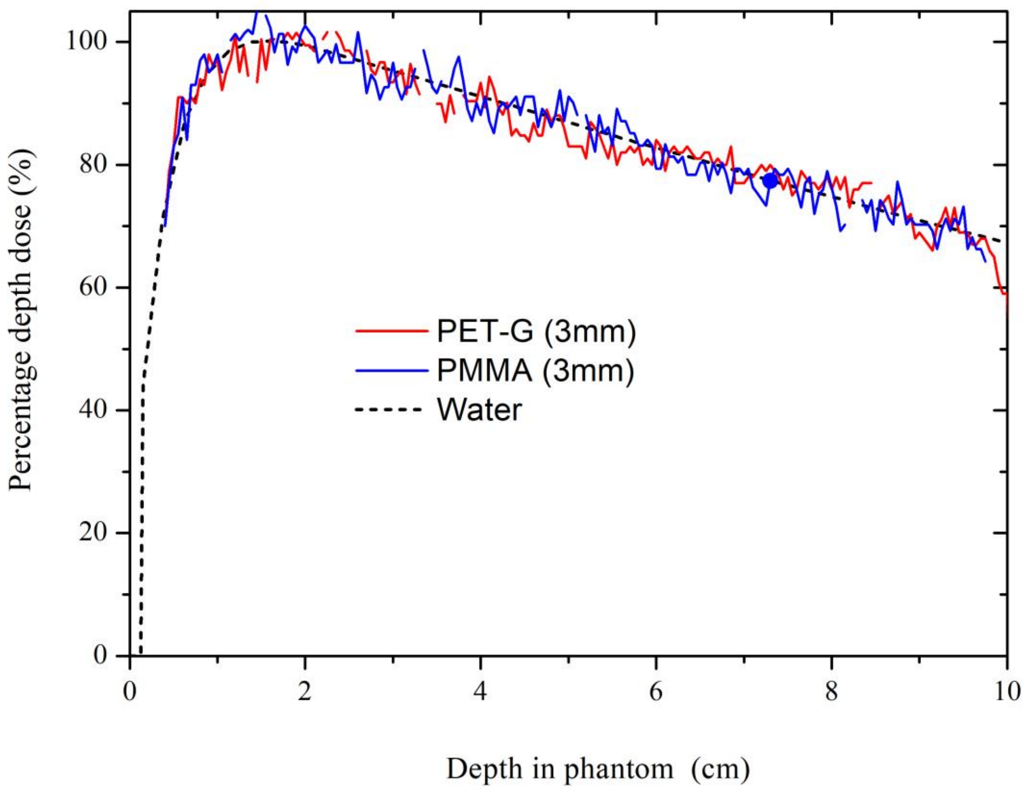

Figure 6: *Comparative chart for 3 mm thick PMMA and PETG plates.*

When the PMMA and PETG plates were positioned in the simulator object, the behaviour of the PDD curves obtained using radiochromic film is similar to all evaluated thicknesses. Yet, the curves have the same behaviour of water related PDD, which were obtained from the radiotherapy service, where the experiment occurred, in conditions like ours.

The maximum uncertainty value associated with each point of PDD found for PETG plates with 1, 2 and 3 mm thick were, respectively, 3%, 6% and 3%; for plates of PMMA, those values were, respectively, 5%, 7% and 9%.

To analyse collected data and compare them, one of the used methods was identifying the maximum and minimum intervals of each plate PDD. This way, it was possible to study if the interval of each PETG plate suits the interval found for the material that had already been used. Table 2 displays data from such intervals in relation to the material that had been used.

Table 2: Table of percentage depth dose (PDD) intervals.

	PDD Intervals	
Plates	**Maximum (%)**	**Minimum (%)**
1 mm PETG	100	71
1 mm PMMA	95	64
2 mm PETG	98	54
2 mm PMMA	97	53
3 mm PETG	98	66
3 mm PMMA	98	63

Considering the maximum uncertainty values, it could be noticed that the minimum and maximum percentage depth dose of the 2 and 3 mm thick PETG plates are closer to those of PMMA plates. With this analysis, it is possible to observe that the usage of PETG in intraoral prosthesis will not result in dose excess not even in dose loss. Throughout the comparison, maximum and minimum values were superior in 1 mm thick PETG plates than in 1 mm thick PMMA plates.

Aiming to study the behaviour in the depth mark where PMMA and PETG plates were positioned – 3 cm deep –, analysis of the percentage dose was made in an interval between 1 mm before and after each plate. To do so, the simple mean of percentages dose of 5 points was calculated, being those points between 2.9 cm and 3.1 cm. In 1 mm thick plates, a difference of 3% was found; in 2 mm thick plates, a difference of 8% was found; and in 3 mm thick plates, a difference of 4% dose was found.

In the last paragraph, percentage dose differences may identify increase/decrease with a positive or negative percentage value of the mean for percentage depth dose in points close to the plates. Results show that uncertainties are of 6%, 9% and 9% for 1, 2 and 3 mm thick plates, respectively. Therefore, the different percentage dose found in the depth in which plates are located is appropriate.

4. CONCLUSION

The study demonstrated similarity up to 7% between PMMA and PETG materials regarding dose distribution in depth when submitted to a 6 MV beam, despite its similar characteristics, as shown in table 1.

The percentage depth dose value surrounding the position of the plates in the simulator object showed values up to 8% of difference between plates within the same dimensions. From the data collected it became possible to infer the existence of similarity in dosimetry behaviour when using PETG for manufacturing intraoral prosthesis for radiotherapy treatments due to its simple handling and low cost, being a substitute to PMMA.

Study limitations: This study compared circular disc plates without analysing dosimetry behaviour in the equipment design, what depends on the anatomic area that will be irradiated.

REFERENCES

[1] NUTTING, C. Radiotherapy in head and neck cancer management: United Kingdom National Multidisciplinary Guidelines. **J Laryngol Otol,** v. 130, n. S2, p. S66-S67, 2016.

[2] MENDENHALL, W. M.; FOOTE, R. L.; SANDOW, P. L.; FERNANDES, R. P. Oral Cavit. In: GUNDERSON, L. L.; TEPPER, J. E. (Eds.) **Clinical Radiation Oncology.** Philadelphia: Elsevier, 2016. p. 570-596.

[3] NEKHLYUDOV, L.; LACCHETTI, C.; DAVIS, N. B.; GARVEY, T. Q.; GOLDSTEIN, D. P.; NUNNINK, J. C.; NINFEA, J. I. R.; SALNER, A. L.; SALZ, T.; SIU, L. L. Head and Neck Cancer Survivorship Care Guideline: American Society of Clinical Oncology Clinical Practice Guideline Endorsement of the American Cancer Society Guideline. **J Clin Oncol,** v. 35, n. 14, p. 1606-1621, 2017.

[4] SAMSON, D. J.; RATKO, T. A.; ROTHENBERG, B. M.; BROWN, H. M.; BONNELL, C. J.; ZIEGLER, K. M.; ARONSON, N. Comparative effectiveness and safety of radiotherapy treatments for head and neck cancer. **AHQR Comparative Effectiveness Reviews,** n. 20, 2010.

[5] SHELLENBERGER, T. D.; WEBER, R. S. Multidisciplinary team planning for patients with head and neck cancer. **Oral Maxillofac Surg Clin North Am,** v. 30, n. 4, p. 435-444, 2018.

[6] MIGLIORATI, C. A.; SENEDA, L. M.; BURTON, E. L. Oral complications of cancer therapy: a summary guide for the clinician. **J Tenn Dent Assoc,** v. 95, n. 1, p. 24-32; quiz 33-4, 2015.

[7] SROUSSI, H. Y.; EPSTEIN, J. B.; BENSADOUN, R.; SAUNDERS, D. P.; LALLA, R. V.; MIGLIORATI, C. A.; HEAIVILIN, N.; ZUMSTEG, Z. S. Common oral complications of head and neck cancer radiation therapy: mucositis, infections, saliva change, fibrosis, sensory dysfunctions, dental caries, periodontal disease, and osteoradionecrosis. **Cancer Med,** v. 6, n. 12, p. 2918-2931, 2017.

[8] KUFTA, K.; FORMAN, M.; SWISHER-MCCLURE, S.; SOLLECITO, T. P.; PANCHAL, N. Pre-radiation dental considerations and management for head and neck cancer patients. **Oral Oncology,** v. 76, p. 42-51, 2018.

[9] OLSON, A.; PHILLIPS, K.; ENG, T.; LENARDS, N.; HUNZEKER, A.; LEWIS, D.; BAUMANN, D. Assessing dose variance from immobilization devices in VMAT head and neck treatment planning: a retrospective case study analysis. **Med Dosim,** v. 43, n. 1, p. 39-45, 2018.

[10] KAANDERS, J. H.; FLEMING, T. J.; ANG, K. K.; MAOR, M. H.; PETERS, L. J. Devices valuable in head and neck radiotherapy. **Int J Radiat Oncol Biol Phys,** v. 23, n. 3, p. 639-45, 1992.

[11] WESSON, R. A.; GARDEN, A. S.; CHAMBERS, M. S. Fabrication of an unconventional bolus-type stent for a combined intraoral/extraoral defect treated with proton radiation therapy. **J Prosthet Dent,** v. 117, n. 4, p. 563-565, 2017.

[12] APPENDINO, P.; FERRERA, F. D.; NASSISI, D.; BLANDINO, G.; GINO, E.; SOLLA, S. D.; REDDA, M. G. R. Are intraoral customized stents still necessary in the era of Highly Conformal Radiotherapy for Head & Neck cancer? Case series and literature review. **Rep Pract Oncol Radiother,** v. 24, n. 5, p. 491-498, 2019.

[13] MARTINS, L. J. O.; BORGES, A. F. S.; FERREIRA, G. Z.; SANSAVINO, S. Z.; SIOSAKI, A. T. F.; TABATA, A.; SANTOS, P. S. S. Material selection for constructing an intraoral stent used in radiotherapy: analysis of density and structure. **Br J Med Med Res,** v. 16, n. 9, p. 1-6, 2016.

[14] NGUYEN, C. T.; LEE, V. S.; WU, J. An acrylic immobilization bite block for use during radiation therapy: description of a new technique. **Int J Prosthodont,** v. 31, n. 4, p. 338-341, 2018.

[15] VERRONE, J. R.; ALVES, F. A.; PRADO, J. D.; MARCICANO, A. D.; PELLIZZON, A. C. A.; DAMASCENA, A. S.; JAGUAR, G. C. Benefits of an intraoral stent in decreasing the irradiation dose to oral healthy tissue: dosimetric and clinical features. **Oral Surg Oral Med Oral Path Oral Radiol,** v. 118, n. 5, p. 573-578, 2014.

[16] HOLLOWS, P.; HAYTER, J. P.; VASANTHAN, S. The Leicester radiotherapy bite block: an aid to head and neck radiotherapy. **Br J Oral Maxillofac Surg,** v. 39, n. 1, p. 49-51, 2001.

[17] IKAWA, H.; KOTO, M.; EBNER, D. K.; TAKAGI, R.; HAYASHI, K.; TSUJI, H.; KAMADA, T. A custom-made mouthpiece incorporating tongue depressors and elevators to reduce radiation-induced tongue mucositis during carbon-ion radiation therapy for head and neck cancer. **Pract Radiat Oncol,** v. 8, n. 2, p. e27-e31, 2018.

[18] FENG, Z.; WANG, P.; GONG, L.; XU, L.; ZHANG, J.; ZHENG, J.; ZHANG, D.; TIAN, T.; WANG, P. Construction and clinical evaluation of a new customized bite block used in radiotherapy of head and neck cancer. **Cancer Radiother,** v. 23, n. 2, p. 125-131, 2019.

[19] BODARD, A. G.; RACADOT, S.; SALINO, S.; POMMIER, P.; ZROUNBA, P.; MONTBARBON, X. A new, simple maxillary-sparing tongue depressor for external mandibular radiotherapy: a case report. **Head Neck,** v. 31, n. 11, p. 1528-30, 2009.

[20] DOI, H.; TANOOKA, M.; ISHIDA, T.; MORIDERA, K.; ICHIMIYA, K.; TARUTANI, K.; KITAJIMA, K.; FUJIWARA, M.; KISHIMOTO, H.; KAMIKONYA, N. Utility of intraoral stents in external beam radiotherapy for head and neck cancer. **Rep Pract Oncol Radiother,** v. 22, n. 4, p. 310-318, 2017.

[21] BOCHNIG, M. S.; OH, M. J.; NAGEL, T.; ZIEGLER, F.; JOST-BRINKMANN, P. G. Comparison of the shock absorption capacities of different mouthguards. **Dent Traumatol,** v. 33, n. 3, p. 205-213, 2017.

[22] SARAC, R.; HELBIG, J.; DRAGER, J.; JOST-BRINKMANN, P. G. A comparative study of shock absorption capacities of custom fabricated mouthguards using a triangulation sensor. **Materials (Basel),** v. 12, n. 21, 2019.

[23] AHN, H. W.; HA, H. R.; LIM, H. N.; CHOI, S. Effects of aging procedures on the molecular, biochemical, morphological, and mechanical properties of vacuum-formed retainers. **J Mech Behav Biomed Mater,** v. 51, p. 356-66, 2015.

[24] ELKHOLY, F.; MIKHAIEL, B.; REPKY, S.; SCHMIDT, F.; LAPATKI, B. G. Effect of different attachment geometries on the mechanical load exerted by PETG aligners during derotation of mandibular canines: an in vitro study. **J Orofac Orthop,** v. 80, n. 6, p. 315-326, 2019.

[25] AMARAL, L. L. **Programa de controle de qualidade dosimétrico, validado com auxílio de filme radiocrômico, aplicado à Radioterapia Estereotáxica.** 2012. 84f. Dissertação (pós-graduação em Física Aplicada à Medicina e Biologia) – Universidade de São Paulo, Ribeirão Preto, 2012.

[26] LUVIZOTTO, J. **Caracterização do filme radiocrômico Gafchromictm modelo EBT3 para uso em braquiterapia.** 2015. 103f. Dissertação (mestrado em Ciências na Área de Tecnologia Nuclear – Reatores) – Instituto de Pesquisas Energéticas e Nucleares, São Paulo, 2015.

[27] CASOLARO, P.; CAMPAJOLA, L.; BREGLIO, G.; BUONTEMPO, S.; CONSALES, M.; CUSANO, A.; CUTOLO, A.; CAPUA, F. D.; FIENGA, F.; VAIANO, P. Real-time dosimetry with radiochromic films. **Sci Rep,** v. 9, art. n. 5307, 2019.

[28] DEVIC, S.; SEUNTJENS, J.; SHAM, E.; PODGORSAK, E. B.; SCHMIDTLEIN, C. R.; KIROV, A. S.; SOARES, C. G. Precise radiochromic film dosimetry using a flat-bed document scanner. **Rev Bras Fis Med,** v. 12, n. 3, p. 7-14, 2005.

[29] NIROOMAND-RAD, A.; BLACKWELL, C. R.; COURSEY, B. M.; GALL, K. P.; GALVIN, J. M.; MCLAUGHLIN, W. L.; MEIGOONI, A. S.; NATH, R.; RODGERS, J. E.; SOARES, C. G. Radiochromic film dosimetry: recommendations of AAPM Radiation Therapy Committee Task Group 55. American Association of Physicists in Medicine. **Med Phys,** v. 25, n. 11, p. 2093-115, 1998.

[30]ALSSABBAGH, M.; TAJUDDIN, A. A.; MANAP, M. B. A.; ZAINON, R. (2017). Evaluation of nine 3D printing materials as tissue equivalent materials in terms of mass attenuation coefficient and mass density. **Ijaas**, v.4, n9, p. 168-173, 2017.

[31] ALVA-SÁNCHEZ, M. S.; DE OLIVEIRA, L. N. ; PETCHEVIST, P. C.; MOREIRA, M. V. ; DE ALMEIDA, A. Beta planar source quality assurance with the Fricke xylenol gel dosimeter. **Radiat. Phys. Chem**, v. 96, p. 56-59, 2014.

[32] BIRNBACHER, L.; WILLNER, M.; MARSCHNER, M.; PFEIFFER, D.; PFEIFFER, F.; HERZEN, J. Accurate effective atomic number determination with polychromatic grating-based phase-contrast computed tomography. **Opt Express**. v.26, n.12, p. 15153-15166, 2018.

[33] SINGH, V. P.; BADIGER,N. M. ; KUCUK, N. Determination of Effective Atomic Numbers Using Different Methods for Some Low-Z Materials. **J Inorg Nucl Chem,** v. 2014, Article ID 725629, p. 1-7, 2014.

[34] Alva, M; PIANOSCHI, T ; Marques, T ; M, M Santanna ; Baffa, O ; Nicolucci, P . Monte Carlo Simulation of MAGIC- f gel for Radiotherapy using PENELOPE. **J Phys Conf Ser**, v. 250, p. 012067, 2010.

[35] MARINI, G. **Avaliação de distribuições de dose em tratamentos radioterápicos utilizando filmes radiocrômicos.** 2013. 75f. Dissertação (mestrado em Física Aplicada à Medicina e Biologia) – Universidade de São Paulo, Ribeirão Preto, 2013.